Received: 23 March 2018 | Revised: 4 June 2018 | Accepted: 8 June 2018

DOI: 10.1002/rra.3319

RESEARCH ARTICLE

WILEY

Regional flood frequency analysis in the central-western river basins of Argentina

Carolina Lauro[1] | Alberto I.J. Vich[1,2] | Stella Maris Moreiras[1,3]

[1]IANIGLA-CCT-Mendoza, Mendoza, Argentina

[2]UNCUYO-Facultad de filosofía y Letras, Mendoza, Argentina

[3]UNCUYO-Facultad de Ciencias Agrarias, Mendoza, Argentina

Correspondence
Carolina Lauro, CONICET-CCT-Mendoza, Av. Ruiz Leal s/n Parque Gral. San Martin, Mendoza CP:5500, Argentina.
Email: clauro@mendoza-conicet.gob.ar

Funding information
Secretaría de Ciencia, Técnica y Posgrado de la Universidad Nacional de Cuyo, Grant/Award Number: 06/G708

Abstract

Knowing the probability of occurrence of a flood event is an important issue for water resources planning. At-site probability models require a long extension of hydrological data for robust estimation of low-frequency events. As the mean record length of 25 gauge stations in western river basins of Argentina is 49 years (until 2010), regional models are an interesting tool to determine mountain rivers system dynamics. This study aims to estimate low-frequency quantiles of annual maximum flow in Argentinean western river basins (28°S–37°S) applying regional frequency analysis based on the L-moments method. Besides, mean annual maximum flow of 75 gauge stations (22°S–52°S) was analysed. First, an exploratory data analysis was performed; normality, independence, and randomness were accepted in the 27%, 87%, and 91% of cases, respectively. Increasing trends in annual maximum flows in the north-western and central-western rivers of Argentina were detected, whereas decreasing trends in annual maximum flow in the Patagonian Andes were identified. Base on at-site characteristics and at-site statistics, a homogeneous region of 12 stations with a record period of 568 years was formed. General extreme value was the most appropriate distribution for this homogeneous study region. Estimation accuracy using Monte Carlo simulations was performed. The error bounds were set at 90%, the mean square error was 9.23%, and the relative bias was 1.6%. The regional method performed better than the at-site estimation.

KEYWORDS

Argentina, L-moments, regional frequency analysis, uncertainty

1 | INTRODUCTION

Argentina is a huge country comprising 2,812,588 km^2 of continental surface and 3,700 km of longitudinal extension reason why a great variety of climates and ecosystems exist. The mean streamflow of superficial water resources is 26,000 m^3/s; although this value has an uneven distribution in the territory, 85% of this streamflow belongs to the La Plata River basin, 7.52% to Patagonian basins, 1.24% to Colorado River system, and 4.69% to basins with drainage to the Pacific Ocean (INCyTH-UNESCO, 1994).

Water resources along the territory have seasonal, interannual and decadal variability. The occurrence of extreme events is more frequent in the last decades due to the global climatic phenomena and human activities (Calcagno, Mendiburu, & Gaviño Noviño, 2000; Camilloni & Barros, 2003; Llano & Penalba, 2011; Paoli & Malinow, 2010). These changes on fluvial system regime affect the water supply for agriculture, industry, energy production, and social activities in general. Due to great impact of these changes on regional economic activities, a detailed analysis of water resources is required.

In Argentina, most studies on flood frequency analysis are conducted for the La Plata River basin, because it is the region of the country more affected by floods. The studies focus on at-site models and the parameters estimation by methods of moments, probability weighted moments, and maximum likelihood, among others (Paoli, Cacik, & Bolzicco, 1995; Paolo, Cacik, & Bolzicco, 1998). However, for the basins located on the western side of the country, there is a

lack of floods characterization, in spite of the problems reported as a result of floods in 1982–1983, 1988–1989, and 1996–1997 periods (Poblete & Escudero, 2013; Poblete & Iranzo, 2012).

The central-western river basins (28°S–37°S) drain an area of 238,748 km^2 with more than 2.6 million of inhabitants. The existing hydraulic infrastructures have eventually cushioned these extreme hydrological events reducing the economic and social impacts. However, in a climatic and land-use change framework, the updated analysis of stream flood frequency is essential to face the vulnerability of productive sectors and population.

The aim of the present work is to estimate low-frequency quantiles of annual maximum streamflow in the Cuyo region (28°S–37°S) performing the method of regional frequency analysis based on L-moments (RFFA-L). Although this method has been successfully applied worldwide such as in the Unites States (Vogel, Thomas, & McMahon, 1993), Australia (Pearson, McKerchar, & Woods, 1991), Pakistan (Hussain, 2011; Hussain & Pasha, 2009), Italy (Noto & La Loggia, 2009), South Africa (Kjeldsen, Smithers, & Schulze, 2002), and West Africa (Kossi, Amisigo, Diekkrüger, & Hountondji, 2016), among others, it has not been a popular tool in our country and only has been applied for the study of annual and seasonal flows (Vich, Norte, & Lauro, 2014). Certainly, this study will contribute to filling the gap knowledge about streamflow extreme events in this region. Besides, it will contribute to understanding the hydrological flood characteristics, which is important for the optimization of water resources planning.

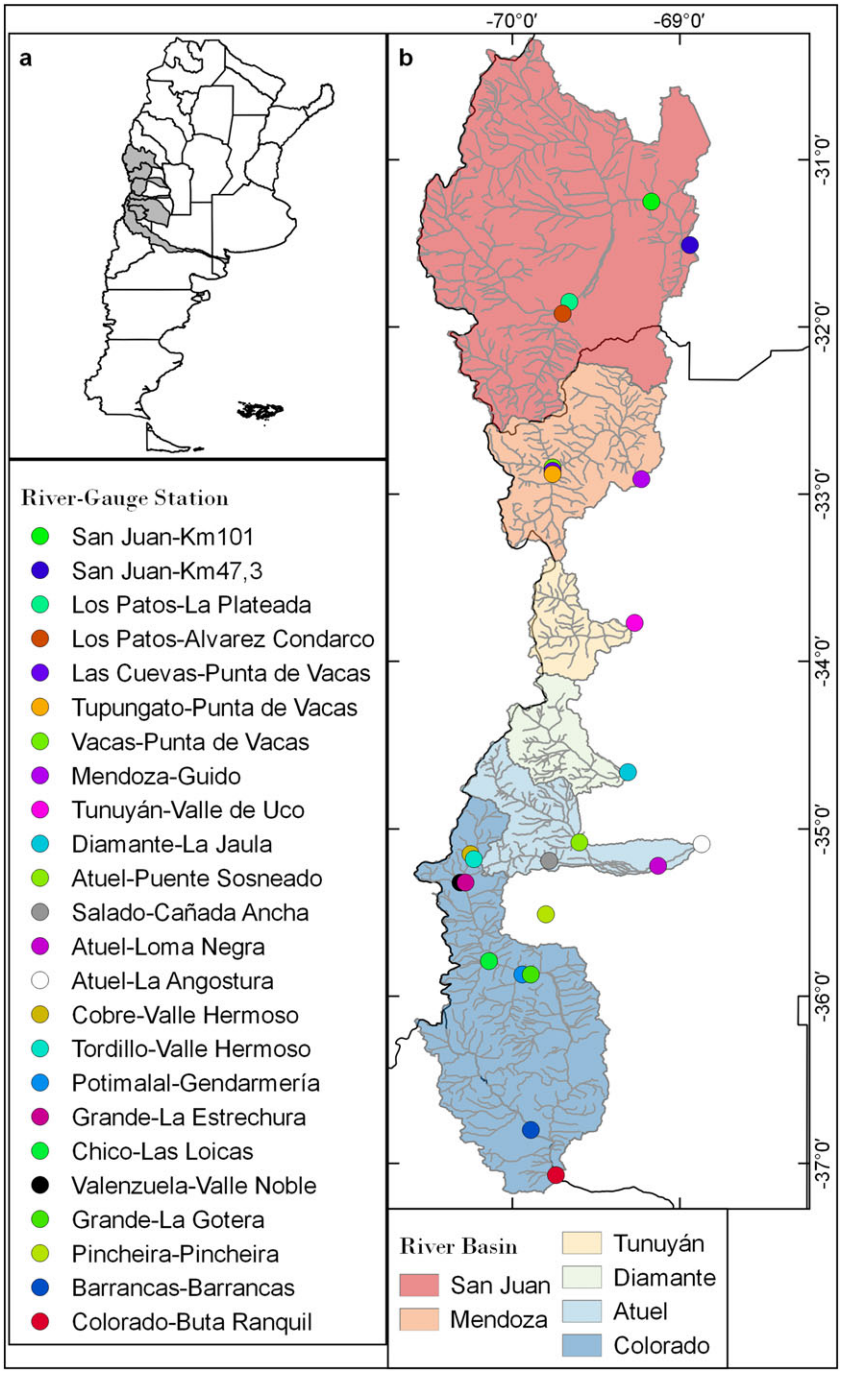

FIGURE 1 (a) Colorado River system. (b) Gauge stations of basins that integrate the Colorado River system, which are the focus of analysis [Colour figure can be viewed at wileyonlinelibrary.com]

2 | STUDY AREA

The study area includes the basins located in the Central West of Argentina between 28°S and 37°S known as Colorado River drainage system (Figure 1a,b). From North to South has approximately 1,000 km of extension integrated by eight important river basins: Jáchal, San Juan, Mendoza, Tunuyán, Diamante, Atuel, Grande, and Colorado. The headwaters of these basins are located on the eastern slope of the Andes Mountain, which has some peaks higher than 5,000 m asl. Topography decreases from West to East losing altitude being slopes gentler to the East. The drainage system is collected by the Desaguadero River. The maximum precipitation (snowfall) occurs in winter over the higher elevations of the Andes; consequently, the streamflow of these basins is fed by snow melting and glacial ablation during the summer season. The hydrological regime is unimodal from July to June. Sixty-six percent to 76% of the flow is during the Spring–Summer season (October to March), whereas, in the winter season, the flow represents only the 9–17%. The annual minimum flow is from June to August, and the annual maximum flow is from November to February.

3 | DATA AND METHODS

3.1 | Streamflow records

Daily streamflow of 75 gauge stations located on western of Argentina between 22°S and 52°S was analysed (Figure 2). The record length of the selected stations is between 18 and 108 years (Table 1). Data were taken from the data base of National River Resources Subsecretary of Argentina.

3.2 | Regional flood frequency analysis

Regional probabilistic models using the hydrological information available on a wide geographic space alleviate the temporary deficit with the spatial abundance of information. As a result, the estimates are robustness than at-site models, which require long extension and quality of data series (Hosking & Wallis, 1997).

The streamflow record period of gauges in basins of the Cuyo region (28°S–37°S) covers a short range (49 years, until 2010), so a reliable estimation of extreme events is disallowed. Given this information limitation, the application of regional methods is preferable to at-site models.

The steps of the RFFA-L are (a) L-moment computation, (b) exploratory data analysis, (c) identification of the homogenous region, (d) function distribution selection, (e) quantiles estimation, and (f) accuracy of estimation.

Finally, a comparison between the at-site and the regional method was done.

3.2.1 | L-moment computation

The L-moments are robust to outliers and virtually unbiased for small samples, making them suitable for flood frequency analysis, including identification of distributions and parameter estimation (Hosking & Wallis, 1997; Vogel & Fennessey, 1993), and are defined as linear combinations of probability weighted moments (Greenwood, Landwehr, Matalas, and Wallis, 1979). Estimation is based on a sample of size N, arranged in ascending order. Let $x(i) < \ldots < x(N_k)$, $(i = 1 \ldots N_k)$ the ordered sample. The unbiased estimator is

$$B_r = \frac{1}{N_k}\sum_{i=1}^{N_k}\frac{(i-1)\ldots(i-r)x_i}{(N_k-1)\ldots(N_k-r)} \quad r = 0, 1, 2, 3, \ldots(Nk-1), \tag{1}$$

where x_i is the ith observation in the site i, N_i the number of observation in the site i, and Br the unbiased estimator of order r.

The sample moment is estimated by

$$L_{r+1} = \sum_{i=0}^{r}\left(\frac{(-1)^{r-i}(r+i)!}{(i!)^2(r-i)!}\right)B_i \quad r = 0, 1, 2, 3, \ldots, (N_k-1). \tag{2}$$

The first L-moment L_1 is equal to the mean value of x. The sample L-moment ratios are defined as

$$L\text{-}CV = t_{2^{(i)}} = {}^{L_2}/_{L_1}, \tag{3}$$

$$L\text{-}CS = t_{3^{(i)}} = {}^{L_3}/_{L_2}, \tag{4}$$

$$L\text{-}CK = t_{4^{(i)}} = {}^{L_4}/_{L_2}, \tag{5}$$

where t_2, t_3, and t_4 are L-coefficient of variation (L-cv), L-skewness (L-cs), and L-kurtosis (L-ck), respectively.

3.2.2 | Exploratory data analysis

First, gaps of daily streamflow data were filled with the maintenance of variance extension method (Hirsch, 1982). Second, annual maximum series were constructed. The presence of outliers was tested with Grubbs test (U.S. Army Corps of the Engineers, 2001), Rosner test (EPA, 2000), and the test developed by the Interagency Advisory Committee on Water Data (1982; formerly WCR). Normality was evaluated with the skewness and kurtosis tests (Salas, Delleur, Yevjevich, & Lane, 1980). Runs and Kendall tests were applied for randomness, and independence was evaluated with Bartlett and Von Neumann ratio tests (Kundzewicz & Robson, 2000). The significance level of all the tests was 5%. If at least one of the tests rejects the null hypothesis, then the existing evidence is considered sufficient to accept the alternative hypothesis.

The techniques for trend and step change detection are only mentioned; readers are particularly referred to references for the details. In both cases, the significance level of all the tests was 5%. For trend, detection was used the nonparametric Mann–Kendall test (Hirsch, Snack, & Smith, 1982; Westmacott & Burn, 1997), with two modifications for autocorrelated data (Hamed & Rao, 1998; Yue & Wang, 2002). For step change, detection was applied the nonparametric Taylor (2000) test.

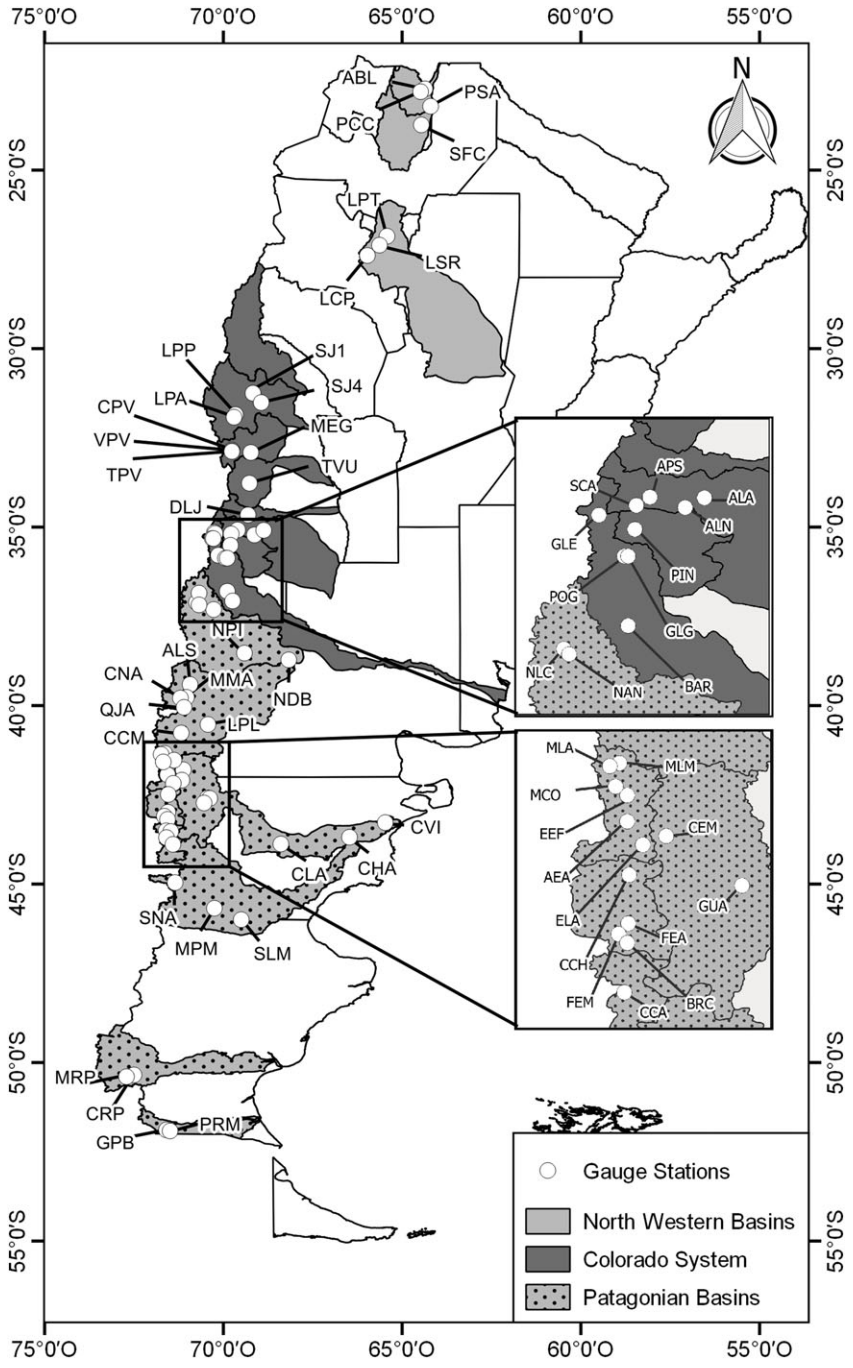

FIGURE 2 Location of gauge stations [Colour figure can be viewed at wileyonlinelibrary.com]

Trend coefficient was estimated by (Hirsch et al., 1982):

$$B = \textit{Median}\left\{\frac{x_j - x_k}{j-k}\right\}\Delta k > j, \tag{6}$$

Where x_j and x_k are sequential data values of the time series in the years i and j. Positive values of the coefficient represent increasing trends, whereas negative values represent decreasing trend.

3.2.3 | Identification of homogeneous region

The aim of this step is to form groups of sites that approximately satisfy the homogeneity condition, that is, the sites frequency distributions are identical apart from a site-specific scale factor.

Two criteria were applied for grouping sites; the first one was considering the geographic position of sites; in this case, first, all sites were grouped together, then were considered two groups: one with sites located above 37.1°S and the other with sites below 37.3°S. This latitude corresponds with the geographic boundary between Patagonia and the rest of the Argentinean territory. The second criterion was to use a cluster approach.

The goal of cluster analysis is to identify clusters of sites with similar characteristics and whose characteristics differ from other group of sites. Two kinds of variables were used: (a) at-site characteristics: latitude, longitude, and elevation of the station, and (2) at-site statistics like L_1, t_2, t_3, t_4, and t_5. Variables were transformed as follow:

$$\text{Gauge station elevation (m.a.s.l)}: Y = \sqrt{(x)}/s.d.\sqrt{(x)}, \tag{7}$$

TABLE 1 Gauge stations characteristics

System	Basin	River	Gauge Station	Initials	Elevation (m asl)	Drainage area (km^2)	Record	Annual maximum flow (m^3/s)
Paraguay	Bermejo	Bermejo	Aguas Blancas	ABL	405	4,850	1944–2011	1,391.4
		Bermejo	Pozo Sarmiento	PSA	296	25,000	1940–2011	4,308.8
		Pescado	Cuatro Cedros	PCC	450	1,700	1956–2011	727.6
		San Francisco	Caimancito	SFC	367	25,800	1946–2011	1,223.8
Laguna Mar Chiquita	Sali-Dulce	Lules	Potrero de las tablas	LPT	950	600	1953–2011	83.4
		Los Sosas	Ruta pcial 187	LSR	650	620	1953–2011	60.0
		Las Cañas	Potrero del Clavillo	LCP	1,300	1,000	1953–2011	56.8
Colorado	San Juan	San Juan	Km101	SJ1	1,310	18,348	1971–2011	194.6
		San Juan	Km47.3	SJ4	945	25,670	1951–2011	169.7
		Los Patos	La Plateada	LPP	1,900	8,500	1951–2011	166.6
		Los Patos	Alvarez Condarco	LPA	1,950	3,710	1951–2011	73.6
	Mendoza	Vacas	Punta de Vacas	VPV	2,450	570	1949–2011	16.2
		Cuevas	Punta de Vacas	CPV	2,430	680	1949–2011	21.0
		Tupungato	Punta de Vacas	TPV	2,450	1,800	1949–2011	85.4
		Mendoza	Guido	MEG	1,550	8,180	1956–2011	149.6
	Tunuyán	Tunuyán	Valle de Uco	TVU	1,200	2,380	1944–2011	92.8
	Diamante	Diamante	La Jaula	DLJ	1,500	2,753	1971–2011	102.7
	Atuel	Atuel	El Sosneado	APS	1,580	2,385	1972–2011	121.3
		Atuel	Loma Negra	ALN	1,340	3,860	1982–2011	95.8
		Atuel	La Angostura	ALA	1,200	3,800	1931–2011	87.8
		Salado	Cañada Ancha	SCA	1,700	810	1939–2011	37.4
	L. Llancanello	Pincheira	Pincheira	PIN	1,750	160	1967–2011	20.0
	Grande	Cobre	Valle Hermoso	CVH	2,150	189	1950–1978	35.8
		Tordillo	Valle Hermoso	TVH	2,200	190	1950–1975	37.4
		Valenzuela	Valle Noble	VVN	1,680	243	1977–2011	37.7
		Chico	Las Loicas	CLL	1,500	220	1991–2011	56.5
		Poti Malal	Puesto Gendarmería	POG	1,485	840	1971–2011	31.2
		Grande	La Estrechura	GLE	1,690	1,070	1977–2011	127.8
		Grande	La Gotera	GLG	1,400	6,180	1971–2011	391.5
	Barrancas	Barrancas	Barrancas	BAR	950	2,900	1960–2011	117.0
	Colorado	Colorado	Buta Ranquil	CBR	850	15,300	1939–2011	486.7
Patagonia	Currileuvú	Currileuvu	Los Maitenes	CLM	959	2,131	1989–2011	15.5
	Neuquén	Nahueve	Los Carrizos	NLC	1,150	1,280	1974–2011	390.4
		Neuquén	Varvarco	NVA	1,180		1981–2011	704.8
		Neuquén	Andacollo	NAN	1,000		1971–2011	732.5
		Neuquén	Paso de Indios	NPI	498	30,843	1902–2011	1935.7
		Neuquén	Dique Ballester	NDB	270		1990–2011	549.6
	Limay	Aluminé	La Siberia	ALS	1,190		1978–2011	969.7
		Malleo	Malleo	MMA	800		1973–2011	191.9
		Chimehuin	Naciente	CNA	875	790	1971–2011	236.8
		Qilquihue	Junin de Los Andes	QJA	750		1962–2011	148.8
		Limay	Paso Limay	LPL	538	26,400	1903–2011	2321.6
		Cuyin Manzano	Cuyin Manzano	CCM	675		1971–2011	107.6
	Chubut	Alto Chubut	Nacimiento	ACN	950	412	1967–2011	41.7
		Chubut	El Maitén	CEM	680	1,200	1943–2011	125.8
		Chubut	Gualjaina	CGU	440	11,055	1990–2011	219.3
		Chubut	Los Altares	CLA	275	16,400	1943–2011	250.0
		Chubut	Valle Inferior	CVI	11	31,681	1993–2011	70.4
		Chubut	Ameghino	CHA	75	29,400	1992–2011	74.4
		Gualjaina	Gualjaina	GUA	510	2,800	1956–2011	90.4
		Lepa	Gualjaina	LGU	498	1,168	1956–2011	1430.9
		Senguer	Nacimiento	SNA	925	1,300	1952–2011	102.1
		Senguer	Los Molinos	SLM	320	17,650	1987–2011	185.7
		Mayo	Paso Mayo	MPM	425	5,450	1980–2011	84.3
	Pacífico	Villegas	Ruta Nac N° 258	VRN	260	60	1959–1985	58.8
		Escondido	El Foyel	EEF	440	153	1977–2011	58.8
		Raquel	El Azul	REA	390	82	1993–2011	20.1
		Azul	Azul	AEA	290	395	1970–2011	153.9
		Epuyén	La Angostura	ELA	290	500	1951–2011	61.4
		Manso	Los Moscos	MLM	792	580	1946–2011	111.0
		Manso	Los Alerces	MLA	728	750	1951–2011	137.1
		Manso	Lago Steffen	MLS	505	1,260	1956–2011	278.7
		Manso	Confluencia	MCO	400	1,815	1965–2011	287.8
		Carrileufú	Choila	CCH	535	580	1957–2011	226.0
		Fontana	Estancia Amancay	FEA	650	47	1956–2011	8.4
		Futaleufú	Embalse Futaleufú	FEM	320	4,608	1979–2011	887.9
		Bagglits	Ruta a Chile	BRC	460	70	1977–2011	17.9
		Hielo	Confluencia	HCO	435	891	1964–2011	182.7
		Huemul	Corcovado	HUC	440	273	1990–2011	27.2
		Carrenleufú	Carrenleufú	CCA	435	2,298	1963–2011	228.2
		Carrenleufú	Lago Vintter	CLV	850	790	1954–2011	61.1

(Continues)

TABLE 1 (Continued)

System	Basin	River	Gauge Station	Initials	Elevation (m asl)	Drainage area (km^2)	Record	Annual maximum flow (m^3/s)
	Santa Cruz	Centinela	Ruta Prov. N° 70	CRP	275	516	1993–2011	37.5
		Mitre	Ruta Prov. N° 11	MRP	200	138	1993–2011	37.4
	Gallegos	Gallegos	Puente Blanco	GPB	610	110	1993–2011	175.2
		Penitentes	Rincón los Morros	PRM	88	138	1993–2011	103.6

$$\text{Gauge station latitude (m)}: Y = x/s.d.(x), \tag{8}$$

$$\text{Gauge station longitude (m)}: Y = x/s.d.(x). \tag{9}$$

Average linkage algorithm was applied. The criterion to select the groups was to consider 25% of Euclidean distance using the hierarchical structure from the dendrograms.

Then it was tested if there was some discordant site to be removed from the region. The discordance measure (Hosking & Wallis, 1993) was applied. This is useful to identify sites that are grossly discordant with the group as a whole. Discordance is measured in terms of L-moments and for the site i is defined as

$$D_i = \frac{1}{3} N (u_i - \bar{u})^T A^{-1} (u_i - \bar{u}), \tag{10}$$

$$A = \sum_{j=1}^{N} (u_j - \bar{u})(u_j - \bar{u})^T, \tag{11}$$

$$\bar{u} = N^{-1} \sum_{i=1}^{N} u_i, \tag{12}$$

where u_i is a vector containing the L-cv, L-cs, and L-ck for a site i, N is the number of sites in the region, $\bar{u}$ is the regional average for u_i, **A** the matrix of sum of squares and cross products.

D_i is compared with a critical value D_c tabulated by Hosking and Wallis (1993), which depends of the number of sites in the region. If $D_i > D_c$, the site is discordant.

The homogeneity of the region was evaluated by the heterogeneity test developed by Hosking and Wallis (1993), which compares the variability of L-moment ratios for the sites in a region with the L-moment ratios of a homogeneous region obtained from simulation, for a collection of sites with the same record lengths as those in the region. The statistics is based on the L-cv.

$$V_1 = \left\{ \sum_{i=1}^{N} n_i \left(t^{(i)} - t^R \right)^2 / \sum_{i=1}^{N} n_i \right\}^{1/2}, \tag{13}$$

where t is L-cv, n_i site i length, N number of site in the region. Site L-moment denoted by i and regional L-moment denoted by R.

The test for heterogeneity fits a four-parameter Kappa distribution to the regional data set, generates a series of 500 equivalent regions data by numerical simulation, and compares the variability of the L-statistics of the actual region to those of the simulated series.

Calculation of the homogeneity measure requires an estimate of the mean (μ_{V_1}) and standard deviation σ_{V_1} of V. This can be accomplished using simulation. The homogeneity measure is then defined as

$$H_1 = \frac{V_1 - \mu_{V_1}}{\sigma_{V_1}}, \tag{14}$$

where H_1 is the homogeneity statistic. A region can be considered homogeneous (HO) if $H_1 < 1$, possibly heterogeneous if $1 \leq H_1 < 2$, and definitely heterogeneous (HE) if $H_1 \geq 2$ (Hosking & Wallis, 1993).

3.3 | Function distribution selection

Once the homogeneous region is selected, an appropriate distribution needs to be fitted. The candidate distributions were exponential (EXP), gumbel (GUM), normal (NOR), generalized Pareto (GPA), generalized extreme value (GEV), generalized logistic (GLO), lognormal (LNO), and Pearson Type III (PE3). The goodness-of-fit is defined in terms of L-moments and is known as Z-statistic (Hosking & Wallis, 1997):

$$Z^{DIST} = \frac{\tau_4^{DIST} - t_4^R + B_4}{\sigma_4}, \tag{15}$$

$$B_4 = \frac{1}{N_s} \sum_{j=1}^{N_s} \left(t_4^j - t_4^R \right), \tag{16}$$

$$\sigma_4 = \sqrt{\frac{1}{N_s - 1} \left\{ \sum_{j=1}^{N_s} \left(t_{4(j)} - t_4^R \right)^2 - N_{sim} B_4^2 \right\}}, \tag{17}$$

where DIST refers to a candidate distribution, τ_4^{DIST} is the population of L-ck of selected distribution, t_4^R is the regional average sample L-ck, B_4 is the bias of regional average sample L-ck, and σ_4 is the standard deviation of regional average sample L-ck. N_s is the number of simulated regional data sets generated using Kappa distribution in a similar way as for the heterogeneity statistic. The subscript j denotes the jth simulated region obtained in this manner. An adequate fit is considered when Z^{DIST} is close to zero; a reasonable criterion is $|Z^{DIST}| \leq 1.64$.

3.3.1 | Quantiles estimation

After the selection of the frequency distribution, a quantile for a given return period could be estimated with the index flood procedure. Assume that the frequency distributions of all sites are identical, except for a site-specific scale factor; in this study, the mean was used.

Suppose that the region has N sites, with site i having record length ni, sample mean L_1, and sample L-moment ratios t_2^i, t_3^i, t_4^i .... Denote by t_2^R, t_3^R, t_4^R, ... the regional average L-moment ratios, weighted proportionally to the sites record length:

$$t_2^R = \sum_{i=1}^{N} n_i t_{2^{(i)}} / \sum_{i=1}^{N} n_i, \tag{18}$$

$$t_r^R = \frac{\sum_{i=1}^{M} n_i t_{r(i)}}{\sum_{i=1}^{N} n_i}, r = 3, 4, ... \quad (19)$$

Set the regional average mean to 1.

Fit the distribution by equating its L-moment ratios L_1, t_2, t_3, t_4, to the regional average L-moment ratios $L_1^R, t_2^R, t_3^R, \ t_4^R$, calculated above. Denote by $\widehat{q}(F)$ the quantile function of the fitted regional frequency distribution.

The quantile estimates at site i are obtained by combining the estimates of μ_i and $q(F)$. The estimate of the quantile with nonexceedance probability F is

$$\widehat{Q_i}(F) = L_1 \widehat{q}(F). \quad (20)$$

3.3.2 | Accuracy of estimations

To evaluate the accuracy of the estimated quantiles and growth curve, an algorithm based on Monte Carlo simulations was applied (Hosking & Wallis, 1997). The first step is to develop a region, similar to the homogeneous region previously found, that is, in terms of the number of sites, record length at each site, regional average L-moment ratios, heterogeneity, and inter-site dependence. This new region is used as the basis for simulations.

The simulation procedure (Hosking & Wallis, 1997)

1. Specify N and for each of the N sites, its record length (ni), and the L-moments of its frequency distribution.
2. Calculate the parameters of the at-site frequency distributions given their L-moments ratios.
3. For each of M repetitions, generate sample data for each site taking into account the intersite dependence.
4. Apply the L-moment algorithm: estimate the L-moment ratios and regional average L-moment ratios, fit the frequency distribution, and estimate the regional growth curve and quantiles for various nonexceedance probabilities (0.5, 0.9, 0.95, 0.98, 0.99, 0.995, 0.998, 0.999, 0.9995, 0.9998, and 0.9999).
5. Calculate the relative error of the estimated regional growth curve and at-site quantiles and the sums needed to calculate overall accuracy measures. For the mth repetition, site-i quantile estimate for nonexceedance probability F is $\widehat{Q}_{i[m]}(F)$. The relative error of this estimate is $\widehat{Q}_{i[m]}(F) - Q_i(F)/Q_i(F)$. Squaring and averaging over all M repetition, the relative root mean square error, relative and absolute bias are approximated as

$$R_i(F) = \left[M^{-1} \sum_{m=1}^{M} \left(\frac{\widehat{Q}_{i[m]}(F) - Q_i(F)}{Q_i(F)} \right)^2 \right]^{1/2} x100\%, \quad (21)$$

$$B_i(F) = M^{-1} \sum_{m=1}^{M} \left(\frac{\widehat{Q}_{i[m]}(F) - Q_i(F)}{Q_i(F)} \right) x100\%, \quad (22)$$

$$A_i(F) = M^{-1} \sum_{m=1}^{M} \left| \frac{\widehat{Q}_{i[m]}(F) - Q_i(F)}{Q_i(F)} \right| x100\%, \quad (23)$$

where $Q_i(F)$ is the real quantile or simulated for the nonexceedance probability F in the site i. A number of M = 1,000 simulation were done.

The performance of quantile estimation procedure over all the sites in the region: regional average relative error (R^R), regional average relative bias (B^R), and regional absolute relative bias (A^R)

$$R^R(F) = N^{-1} \sum_{i=1}^{N} R_i(F), \quad (24)$$

$$B^R(F) = N^{-1} \sum_{i=1}^{N} B_i(F), \quad (25)$$

$$A^R(F) = N^{-1} \sum_{i=1}^{N} |B_i(F)|. \quad (26)$$

Analogous quantities can be calculated for estimates of growth curve, but with $Q_i(F)$ and $\widehat{Q}_{i[m]}(F)$ replaced by $q_i(F)$ and $\widehat{q}_{i[m]}(F)$, respectively. Ninety percent error bounds for $\widehat{Q}(F)$ are

$$\frac{\widehat{Q}(F)}{U_{0.05}(F)} \le Q(F) \le \frac{\widehat{Q}}{L_{0.05}(F)}. \quad (27)$$

For a particular nonexceedance probability F, it may be found that 5% of the simulated values of $\widehat{Q}(F)/Q(F)$ lie below some value $L_{0.05}$ whereas 5% lie above some value $U_{0.05}$. Then 90% of the distribution of $\widehat{Q}(F)/Q(F)$ lies between the intervals:

$$L_{50}(F) \le \widehat{Q} \le U_{95}(F) \quad (28)$$

3.3.3 | Comparison between at-site and regional quantile estimation

The flow estimated by the regional method results from the product of the avenue index of the regional growth curve by the scale factor, in this case, equivalent to the mean of the site series (Equation (20)). The flow rates of each site that make up the different homogeneous regions were estimated; the mean square error and the confidence interval were calculated with Monte Carlo simulations as explained above. These streamflows were compared with the estimation of the streamflow through the at-site method using L-moments. Monte Carlo simulations were performed for the assignment of the mean square error of the estimation and the error bounds.

4 | RESULTS

4.1 | Data screening

From the 75 analysed gauges, 11 had more than 20% of missing values. Normality, independence, and randomness had been accepted in the 27%, 87%, and 91% of cases, respectively. Outliers were identified in 1953, 1977, 1982, 1984, 1986, 1987, 1988, 1990, 1991, 1992,

TABLE 2 Exploratory data analysis

Initials	Percentage of missing data	Normality	Randomness	Independence	Outliers	Trend	Shift
ABL	0.0	R	A	A	—	9.48	ns
PSA	0.0	R	R	R	—	45.89	1974 +
PCC	2.2	A	A	R	—	0.03	1970 +
SFC	9.6	R	A	A	—	−0.78	1983 −
LPT	9.7	R	A	A	—	−0.09	1986 −
LSR	3.0	R	R	A	—	0.00	ns
LCP	0.0	R	R	A	—	−0.05	ns
SJ1	22.3	R	A	A	1987-84	−0.31	ns
SJ4	0.3	R	A	A	—	0.57	ns
LPP	9.8	R	A	A	—	−0.08	ns
LPA	3.6	R	A	A	—	0.15	ns
VPV	5.4	R	A	A	1987	0.07	ns
CPV	6.6	R	A	A	—	0.12	ns
TPV	5.3	R	A	A	1984	0.36	ns
MEG	0.0	R	A	A	1982	0.83	1976 +
TVU	0.7	R	A	A	—	0.12	ns
DLJ	1.3	A	A	A	—	−0.35	ns
APS	2.2	R	A	A	1992	−0.95	ns
ALN	0.0	A	R	A	1982	−1.41	ns
ALA	0.2	R	A	R	—	0.24	1971 +
SCA	4.3	R	A	A	1992	0.23	1976 +
PIN	12.6	R	A	A	1991-07	0.17	ns
CVH	32.7	A	A	A	1953	−0.44	ns
TVH	40.4	R	A	A	—	−0.31	ns
VVN	25.3	A	A	A	1990	−0.09	ns
CLL	4.2	R	A	A	1998-07	0.69	ns
POG	3.5	A	A	A	1988	−0.20	ns
GLE	16.0	R	A	A	1982	−1.70	ns
GLG	4.7	R	A	A	1992	−0.79	ns
BAR	13.8	R	A	A	1998	0.77	ns
CBR	41.3	R	A	A	—	1.59	1971 +
CLM	13.2	R	A	A	—	−1.54	ns
NLC	5.6	A	A	A	—	0.93	ns
NVA	23.5	A	A	A	2008	−3.80	ns
NAN	6.8	A	A	A	—	−0.34	ns
NPI	0.0	R	R	A	—	7.05	ns
NDB	0.2	R	A	A	2010	−1.90	ns
ALS	19.8	R	A	A	1986-91	−3.38	ns
MMA	7.1	R	A	A	2006	2.19	1999 +
CNA	12.6	R	A	A	2006	0.44	ns
QJA	4.4	R	A	A	1983-05-97	0.71	ns
LPL	11.8	R	A	A	—	−11.23	ns
CCM	9.3	R	A	A	2009	0.27	1992 +
ACN	36.7	R	A	R	1977	−0.15	ns
CEM	0.5	A	R	A	1998	0.05	1982 −
CGU	1.6	R	A	R	2004	−0.38	ns
CLA	2.2	R	A	A	—	0.76	ns
CVI	4.7	R	A	A	—	−1.84	ns
CHA	4.2	A	A	A	—	−0.61	ns
GUA	2.1	R	A	A	—	−0.46	ns

(Continues)

TABLE 2 (Continued)

Initials	Percentage of missing data	Normality	Randomness	Independence	Outliers	Trend	Shift
LGU	43.3	R	R	A	—	−0.68	1986 −
SNA	16.4	R	A	R	—	−0.14	1984 −
SLM	0.0	A	A	A	—	0.75	1990 +
MPM	10.9	R	R	A	1991	2.49	1990 +
VRN	4.0	A	A	A	—	−0.39	1982 −
EEF	2.6	R	A	A	2002-04-09-77	0.79	2001 +
REA	1.6	R	A	A	—	−0.96	ns
AEA	0.2	A	A	A	1988	0.44	ns
ELA	6.6	R	A	A	—	−0.24	ns
MLM	7.7	A	A	A	—	0.17	ns
MLA	3.4	R	A	A	1998	0.55	ns
MLS	50.5	A	A	A	—	0.27	ns
MCO	4.4	R	A	A	—	−1.91	ns
CCH	1.9	R	A	A	—	−0.70	ns
FEA	4.9	R	A	A	—	−0.02	ns
FEM	6.5	R	A	A	—	5.01	ns
BRC	5.2	A	A	A	1995	−0.32	ns
HCO	39.1	R	A	A	—	1.73	1978 +
HUC	3.5	R	A	A	—	−1.47	1997 −
CCA	13.3	R	R	A	1988-91	1.34	ns
CLV	50.9	A	A	A	—	0.11	ns
CRP	0.0	A	R	A	—	−0.69	2003 −
MRP	0.2	R	A	R	1999	−0.09	2001 −
GPB	0.0	A	A	A	2010	−3.88	ns
PRM	0.0	R	A	A	—	3.67	ns

Note. R: Rejects the null hypothesis; A: accept the null hypothesis. In bold significant trend. Ns = nonsignificant step change.

1995, 1998, 1999, 2004, 2006, 2007, 2008, 2009, and 2010 (Table 2). Then these years are coincident with years of moderate and great intensive ENSO events (Nicholls, 2008; Trenberth, 1997). The outliers were not removed from the analysis since the annual maximum flow obtained from averages of a set of more or less important observations, hardly with measurement errors.

A significant trend was detected in 13.3% of cases; most of them were increasing trends. Also, 28% of cases had significant step changes, being mainly positive changes. In north and central-western river basins, the majority of changes were positive during the 1970s (Table 2). Some Patagonian river showed increasing trends while others decreasing trends. Trend detection is conditioned to the initial year selected for the analysis and the data series length. Lack of stationarity could be attributable to natural or to anthropogenic causes even though basins under study have a low anthropic impact such as urbanization or land uses changes.

The L-moment values for all data set are plotted in Figure 3a,b. The L-cv values were between 0.13 and 0.88 with a mean value of 0.31. The L-cs range was between −0.23 and 0.80 with a mean value of 0.25, whereas L-ck range was −0.1 to 0.45 with a mean value of 0.10. In Figure 3, the sites away from the centre of the cloud point were LGU and NDB. The site LGU had neither outlier nor trend, but it had a step change in 1986, whereas the site NDB had an outlier in 2010 but no changes were identified.

4.2 | Homogeneous region

When all sites are considered together resulted in an HE region with three sites discordant, after removing those discordant sites, the region is still HE and other sites resulted discordant. Separating these sites in North and South of parallel 37.1°S and 37.3°S, respectively, no regions resulted homogeneous.

The found region is constituted by geographically continuous sites due to the used methodology, although it is not necessary to fulfil this condition. After applying the cluster analysis, the 75 gauging stations were grouped into 10 regions, being only five of them homogeneous (Figure 4a); the remaining were HE. In the case of the Colorado River system, only one homogeneous region was found composed by 13 gauges belonging to Mendoza (MEG), Tunuyán (TVU), Diamante (DLJ), Atuel with three gauging stations (APS, ALN, and ALA), Salado (SCA), Chico (CLL), Potimalal (POG), Grande (GLE and GLG), Barrancas (BAR), and Colorado (CBR) Rivers (Figure 4b). Finally, the station SCA was removed from the analysis because it did not fulfil the stationarity assumption.

The 12 analysed stations had a total record length of 568 years. According to the criterion of not extrapolating more than five times, the length of the series, for any site within the mentioned region, then a robust estimation of maximum streamflow can be obtained for a return period (T) of 113.6 years.

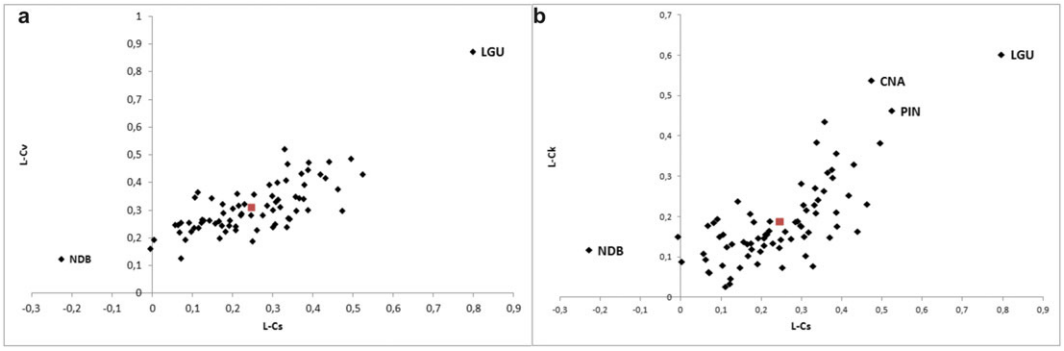

FIGURE 3 (a) L-cv versus L-cs. (b) L-ck versus L-cs. The red square indicates the regional mean L-moment [Colour figure can be viewed at wileyonlinelibrary.com]

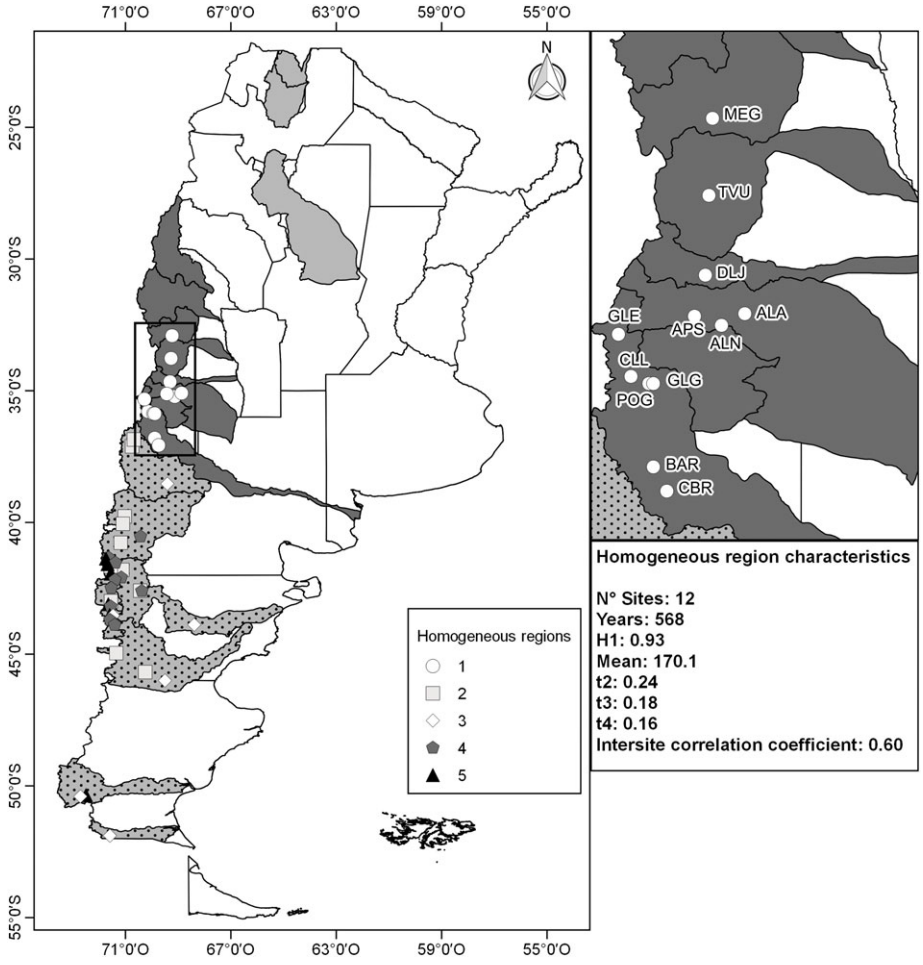

FIGURE 4 (a) Homogeneous regions found in western Argentina. (b) Gauges stations integrating the homogeneous region for Cuyo [Colour figure can be viewed at wileyonlinelibrary.com]

4.3 | Frequency distribution selection, quantile estimation, and accuracy of the estimation

The frequency distribution functions that met the Z^{dist} criteria (<|1,64|) were EXP (0.10), GEV (−0.73), GUM (−0.86), GNO (−1.06), and GLO (1,64) being the exponential function the lowest absolute value.

Then the quantiles, the error bounds, and the bias for the 12 predetermined frequencies (T = 2, 5, 10, 20, 50, 100, 200, 500, 1,000, 2,000, 5,000, 10,000 years) of each function that met the Z^{dist} criteria were calculated. Based on the measure of the regional average of the mean square error (R^R), the most robust model is chosen, being the one whose average for the 12 determined frequencies is smaller. In Figure 5, the values of mean square error (Figure 5a) and bias (Figure 5b) are shown.

The best fitting distribution function turned out to be the GEV, with a regional mean square error of 9.23% and the relative bias of

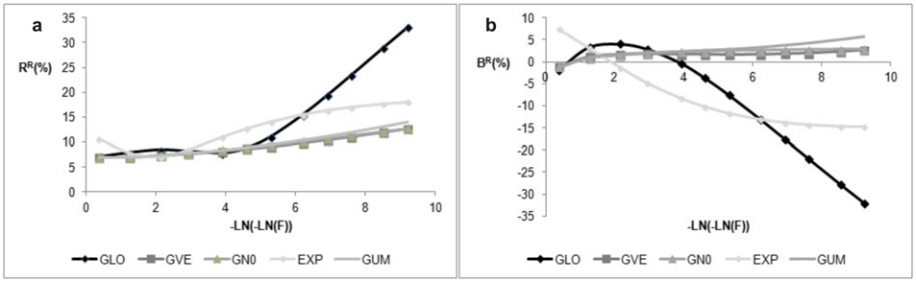

FIGURE 5 (a) Mean square error, the lowest values for the 12 frequencies are for the GEV function. (b) Bias, lowest absolute values are for the GEV function [Colour figure can be viewed at wileyonlinelibrary.com]

TABLE 3 Quantiles estimates for regional growth curve, error, error bounds, and relative bias

T	10,000	5,000	2,000	1,000	500	200	100	50	20	10	5	2
Regional quantile	4.2	3.9	3.6	3.3	3.0	2.7	2.4	2.2	1.9	1.6	1.3	0.9
R^R	12.6	11.9	11.0	10.4	9.8	9.1	8.6	8.2	7.7	7.4	7.1	7.0
$L_{0.05}$	3.6	3.4	3.2	3.0	2.8	2.5	2.3	2.1	1.9	1.6	1.3	0.9
$U_{0.05}$	5.0	4.6	4.1	3.8	3.5	3.0	2.7	2.4	2.0	1.7	1.4	0.9
B^R	2.6	2.3	2.0	1.8	1.7	1.6	1.7	1.7	1.7	1.7	1.1	−1.1

Note. Distribution fitted GEV, parameters ε = 0.79, α = 0.35, κ = −0.01.

2.4%, the uncertainty measures were determined based on the simulation processes of the type of Monte Carlo. Table 3 shows the estimated quantiles for regional growth curve, error, error bounds, and relative bias.

4.4 | Comparison between at-site and regional estimation

The flow estimates with the regional method result from the product of the avenue index of the regional growth curve with a scale factor, in this case, equivalent to the average of the series of the site.

For the homogeneous Cuyo region, the regional estimation was more accurate than at-site estimation; the mean squared error was lower for the 12 frequencies analysed, this difference in extreme frequencies being remarkable (Table 4).

Another feature that allows comparing the robustness of one method with the other is the amplitude of the confidence interval. Being the amplitude smaller for the RFFA-L indicating that is better (Figure 6).

5 | DISCUSSION AND CONCLUSION

The study region is the mountain basins of western Argentina. The development of the cities located in the foothills of the Andes Mountain (28°S–37°S) was possible because of water resources used for agro-industry activities and energy production. In this context, water resources management requires estimates of the probability of occurrence of hydrological variables for decision making, especially for design hydraulic structure to prevent flood hazards. Therefore, the present study consists of estimating flood quantiles, applying a methodology frequently used in different parts of the world but not commonly adopted in Argentina yet.

The prediction of low-frequency events requires large, complete, and homogeneous data series, a fact that is not fulfilled in the most cases of the Cuyo region. This fact introduces a high level of uncertainty in the streamflow estimations. The record period of regional gauges is short in the Andes Mountain Rivers, and in some cases with more than 20% of missing data. Additionally, series are not stationary due to the presence of step changes and trends related to ocean–climate patterns.

According to our findings, the streamflow increase in north-western basins could be related with a growth of summer precipitation rates. Precipitations have increased 49 mm in the period 1960–2010 (Celis et al., 2009).

On the other hand, the streamflow of the Colorado System is more dependent of the snow precipitation during the winter season. In this context, temperature, which has been increasing in the West of Argentina (SAyDS, 2015), has a key role in snow and glacial melting, and consequently in increasing streamflow during summer. Interannual variation of streamflow in the Cuyo Rivers has been linked to variations in sea surface temperature on the Tropical Pacific Ocean (Flamenco & Villalba, 2006; Montecinos & Aceituno, 2003). Meaning

TABLE 4 Ratio of the mean squared error (RMSE) of at-site quantile estimators to regional quantile estimators for the 12 frequencies analysed

F	5,E-01	2,E-01	1,E-01	5,E-02	2,E-02	1,E-02	5,E-03	2,E-03	1,E-03	5,E-04	2,E-04	1,E-04
T	2	5	10	20	50	100	200	500	1000	2000	5000	1,E04
RMSE ratio	1.07	0.95	1.05	1.23	1.58	1.86	1.79	1.62	1.53	1.48	1.47	1.49

Note. Values greater than 1 indicate greater precision of the regional method.

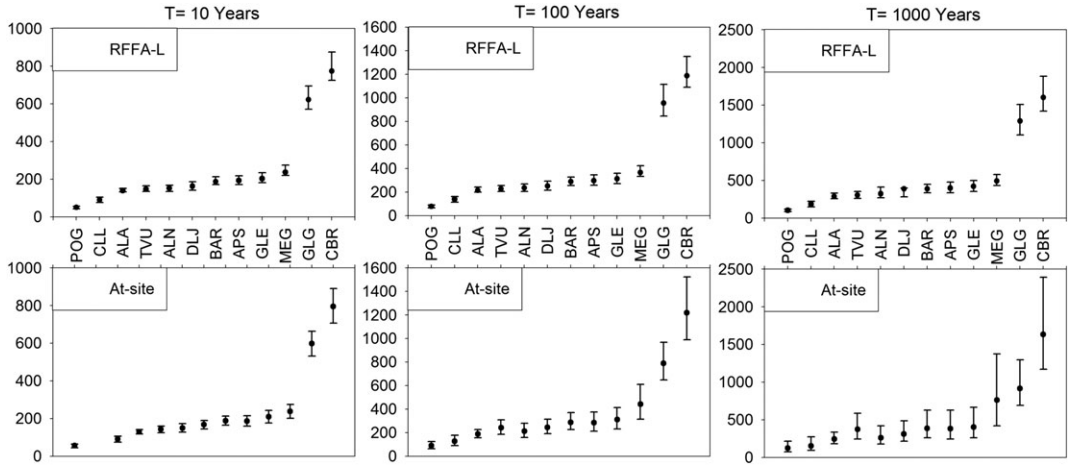

FIGURE 6 For each site of the homogeneous region, the amplitude of intervals for three return periods. In the regional method (top), the intervals are more uniform and have less amplitude than in at-site analysis (bottom)

the warm phase of the ENSO phenomena (El Niño) is associated with higher snow precipitation and higher streamflow, while lower snow precipitation and streamflow are associated with the cold phase of ENSO (La Niña; Masiokas, Villalba, Luckman, Le Quesne, & Aravena, 2006). Also, regimen shifts coincident with the Pacific Decadal Oscillation have been found in streamflow records (Masiokas, Iba, Luckman, & Mauget, 2010).

In Patagonian Rivers, annual maximum flow is originated by precipitation during the austral winter season. The decreasing trends found in annual maximum in this study match with the decreasing trend reported for precipitation in the period 1950–2000 (Aravena & Luckman, 2009; Garreaud, Lopez, Minvielle, & Rojas, 2013).

The regional frequency analysis allows to increase the length of the records, transferring information from different stations of a homogeneous region in order to conduct a more accurate frequency study. Twelve gauge stations were found to be homogeneous meaning that each site has the same parental distribution, except for a scale factor. The found region is approximately similar to the "Cuyo Sur" region identified by Compagnucci and Araneo (2007) based on streamflow variability and its connection with the ENSO phenomenon. Additionally, the region is similar to the homogeneous region found by Vich et al. (2014) for summer streamflow, which represents the highest streamflow period in the Cuyo Rivers. From the found homogeneous region, the streamflow in each particular station can be estimated with greater certainty for events of 128 years of recurrence.

Based on the Z^{dist} statistic, five distributions EXP, GEV, GUM, GLO, and GNO have been identified as suitable candidates for regional analysis. Accuracy measures for the estimated regional growth curves and quantiles have been calculated for the five candidate distributions, using Monte Carlo simulations. These simulations showed that the GEV distribution is the most robust model (lowest errors and biases). Based on these results, the GEV distribution is suggested to be used in order to predict flood quantiles and their associated recurrence intervals for this particular region. Furthermore, these results provide the basis for further applications in ungauged sites of the Cuyo region.

In this study, the regional frequency analysis performs a better result than the at-site analysis, being the mean squared error lower for the regional method. Regional frequency models based on data from a homogeneous region are generally more efficient than at-site models, which are based on singles samples, and efficiently reduce random and climatologically irrelevant variations in the estimates of the model parameters and high quantiles (Cunnane, 1986; Kyselý, Gaála, & Picek, 2011). These findings have been also noted for other mountain rivers as the Indus River in Pakistan that RFFA performs better than at-site analysis (Hussain, 2011).

This finding represents a huge step forward in the local context towards the improvement of flood management. In the context of climate change, future work will focus on frequency analysis of nonstationary observations.

ACKNOWLEDGEMENTS

This research was supported by Secretaría de Ciencia, Técnica y Posgrado de la Universidad Nacional de Cuyo 06/G708 leader by A. Vich. The authors thank the Subsecretaría de Recursos Hídricos (BDHI), Argentina, for providing discharge time series. These results are part of the PhD thesis of Carolina Lauro.

ORCID

Carolina Lauro http://orcid.org/0000-0001-7150-3885

REFERENCES

Aravena, J. C., & Luckman, B. H. (2009). Spatio-temporal rainfall patterns in southern South America. *International Journal of Climatology*, *29*, 2106–2120.

Calcagno, A., Mendiburu, N., & Gaviño Noviño, M. (2000). Informe sobre la gestión del agua en la Republica Argentina. *World Water Vision*.

Camilloni, I., & Barros, V. (2003). Extremes discharges in the Paraná River and their climate forcing. *Journal of Hydrology*, *278*, 94–106.

Celis, A., Ostuni, F., Kisilevsky, G., Schwartz, E., Fernández Bouzo, S., & Lopresti, L. (2009). *Documento País: Riesgos de desastres en Argentina. CAPITULO 5: Cambio climático: variabilidad pasada y una prospectiva de las amenazas de acuerdo a los escenarios futuros*. Buenos Aires: Cruz Roja Argentina, Centro Estudios Sociales y Ambientales.

Compagnucci, R.H., y Araneo, D. (2007) Alcances de El Niño como predictor del caudal de los ríos andinos argentinos. *Ingeniería Hidráulica en México*, *22*(3), 23–35.

Cunnane C. (1986). Review of statistical models for flood frequency estimation. Hydrologic frequency modeling. *Proceeding of the international Symposium on flood frequency and risk analysis*. (pp. 49-96). Louisana State University, Baton Rouge, Ed. Vijay P. Singh. U.S.A.

Environmental Protection Agency (2000). Guidance for data quality assessment. Practical methods for data analysis. EPA QA/G-9. QA00 Update.

Flamenco, E. A., & Villalba, R. (2006). Relationships between sea surface temperatures and streamflows across the Cordillera de los Andes. *Proceedings of 8 ICSHMO*, (pp. 1259–1263). Foz do Iguaçu, Brazil, April 24–28, 2006, INPE.

Garreaud, R., Lopez, P., Minvielle, M., & Rojas, M. (2013). Large-scale control on the Patagonian climate. *Journal of Climate*, *26*(1), 215–230.

Greenwood, J. A., Landwehr, J. M., Matalas, M. C., & Wallis, J. R. (1979). Probability weighted moments: Definitions and relation to parameters of several distributions expressable in inverse form. *Water Resources Research.*, *15*, 1049–1054.

Hamed, K. H., & Rao, A. R. (1998). A modified Mann-Kendall trend test for autocorrelated data. *Journal of Hydrology*, *204*(1–4), 182–196.

Hirsch, R., Snack, J., & Smith, R. (1982). Techniques of trend analysis for monthly water quality data. *Water Resources Research*, *18*(1), 107–121.

Hirsch, R. M. (1982). A comparison of four streamflow record extension techniques. *Water Resources Research*, *18*(4), 1081–1088.

Hosking, J., & Wallis, J. (1993). Some statistics useful in regional frequency analysis. *Water Resources Research*, *29*, 271–281.

Hosking, J., & Wallis, J. (1997). *Regional frequency analysis. An approach based on L-Moments*. U K: Cambridge University.

Hussain, Z. (2011). Application of the regional flood frequency analysis to the upper and lower basins of the Indus River, Pakistan. *Water Resour Manage*, *25*, 2797–2822. https://doi.org/10.1007/s11269-011-9839-5

Hussain, Z., & Pasha, G. (2009). Regional flood frequency analysis of the seven sites of Punjab, Pakistan, using L-moments. *Water Resources Management*, *23*, 1917–1933. https://doi.org/10.1007/s11269-008-9360-7

INCyTH/UNESCO (1994), *Balance Hídrico de la República Argentina*. Citado por: Calcagno, A., Urbano, J.L., Planas, A.C., Gaviño Novillo, M., & Mendiburo, N., *Informe sobre la gestión del Agua en la República Argentina*. Buenos Aires; Global Water Partnership, 2000.141 p.

Interagency Advisory Comite on Water Data (USACE) (1982). Guidelines for determining flood flow frequency. *Bulletin 17 B. U.S. Department of Interior*. Geological Survey. Office of Water Data Coordination.

Kjeldsen, T. R., Smithers, J. C., & Schulze, R. E. (2002). Regional flood frequency analysis in the KwaZulu-Natal province, South Africa using the index-flood method. *Journal of Hydrology*, *255*, 194–211.

Kossi, K., Amisigo, B. A., Diekkrüger, B., & Hountondji, F. C. C. (2016). Regional flood frequency analysis in the Volta River basin, West Africa. *Hydrology*, *3*, 5. https://doi.org/10.3390/hydrology3010005

Kundzewicz, Z., & Robson, A. (2000). *Detecting trend and other changes in hydrological data*. Geneva. WCDMP-45. WMO/TD, 1013

Kyselý, J., Gaála, L., & Picek, J. (2011). Comparison of regional and at-site approaches to modeling probabilities of heavy precipitation. *Int. J. Climatol.*., *31*, 1457–1472.

Llano, M., & Penalba, O. (2011). A climatic analysis of dry sequences in Argentina. *Int. J. Of Climat*., *31*(4), 504–513.

Masiokas, M., lba, R., Luckman, B., y Mauget, S. (2010). Intra-to multidecadal variations of snowpack and streamflow records in the Andes of Chile and Argentina between 30° and 37°S. *Journal of Hydrometeorology*, *11*, 822–831.

Masiokas, M., Villalba, R., Luckman, B. H., Le Quesne, C., & Aravena, J. C. (2006). Snowpack variations in the Central Andes of Argentina and Chile, 1951 – 2005: Large-scale atmospheric influences and implications for water resources in the region. *Journal of Climate*, *19*, 6334–6352.

Montecinos, A., & Aceituno, P. (2003). Seasonality of the ENSO-related rainfall variability in Central Chile and associated circulation anomalies. *Journal of Climate*, *16*, 281–296.

Nicholls, N. (2008). Recent trends in the seasonal and temporal behavior of the El Niño–Southern oscillation. *Geophysical Research Letters*, *35*, L19703. https://doi.org/10.1029/2008GL034499

Noto, V. L., & La Loggia, G. (2009). Use of L-moments approach for regional flood frequency analysis in Sicily, Italy. *Water Resour Manage*, *23*, 2207–2229. https://doi.org/10.1007/s11269-008-9378-x

Paoli, C., Cacik, P., & Bolzicco, J. (1995). Aplicación de métodos robustos para la determinación de máximas crecidas del río Paraná. *Información tecnológica*, *6*(6), 169–178.

Paolo, C., Cacik, P., & Bolzicco, J. (1998). Análisis de riesgo conjunto en la determinación de crecidas de proyecto de regímenes complejos. *Ingeniería del Agua*, *5*(2), 11–20.

Paoli, C., & Malinow, G. (2010). *Criterios para la determinación de crecidas de diseño en sistemas climáticos cambiantes*. Santa Fe: Ediciones UNL.

Pearson, C. P., McKerchar, A. I., & Woods, R. A. (1991). Regional flood frequency analysis of western Australian data using L-moments. *International Hydrology and Water Resources Symposium* (pp. 631–632) Perth, Australia.

Poblete, A. G., & Escudero, S. A. (2013). La sequia en los Andes Centrales y su repercusión en los ríos San Juan y Mendoza. *IV Congreso Nacional de Geografía. XI Jornadas cuyanas de geografía*. ISSN 2346-9698.

Poblete, A. G., & Iranzo, D. A. (2012). Análisis de factores de circulación atmosférica regional y cupla océano-atmósfera que generaron el período nival más seco del siglo XX en los andes centrales de Argentina y Chile. IX *Jornadas Nacionales de Geografía Física*. Bahía Blanca, 19 al 21 abril de 2012.

Salas, J., Delleur, J., Yevjevich, V., & Lane, W. (1980). *Applied modeling of hydrologic time series*. Colorado: Water Resources Publications.

Secretaría de Ambiente y Desarrollo Sustentable de la Nación (SAyDS) (2015). *Tercera Comunicación Nacional de la República Argentina a la Convención Marco de las Naciones Unidas sobre Cambio Climático. Cambio climático en Argentina; tendencias y proyecciones*. Buenos Aires: Secretaría de Ambiente y Desarrollo Sustentable de la Nación.

Taylor, W. (2000). Change-point analysis: A powerful new tool for detecting changes. Retrieved from: http://www.variation.com/cpa/tech/changepoint.html. (Accessed, 15/03/2013).

Trenberth, K. E. (1997). The definition of El Niño. *Bulletin of the American Meteorological Society.*, *78*, 2771–2777.

U.S. Army Corps of the Engineers (2001). Performance evaluation (PE) program. Engineer manual 200–1-7.

Vich, A. I. J., Norte, F., y Lauro, C. (2014). Análisis regional de frecuencias de caudales de ríos pertenecientes a cuencas con nacientes en la Cordillera de los Andes. *Meteorológica*, *39*(1), 3-26.

Vogel, R., & Fennessey, M. (1993). L-moments diagrams should replace moment product diagrams. *Water Resources Research*, *29*, 1745–1752.

Vogel, R. M., Thomas, W. O., & McMahon, T. A. (1993). Flood-flow frequency model selection in southwestern United States. *Journal of Water Resources Planning and Management*, *119*(3), 353–366.

Westmacott, J., & Burn, D. (1997). Climate change effects on the hydrologic regime within the Curchill Nelson River basin. *Journal of Hydrology*, *202*, 263–279.

Yue, S., & Wang, C. Y. (2002). The influence of serial correlation on the Mann-Whitney test for detecting a shift in median. *Advances in Water Resources*, *25*, 325–333.

How to cite this article: Lauro C, Vich AIJ, Moreiras SM. Regional flood frequency analysis in the central-western river basins of Argentina. *River Res Applic*. 2018;1–13. https://doi.org/10.1002/rra.3319